

## COMPUTATION ACCURACY OF ELECTROMAGNETIC WAVE PROPAGATION OVER IRREGULAR TERRAIN

Vladimír SCHEJBAL

The Department of electrical, electronic and safety engineering

### 1. Introduction

Irregular terrain reflection computation for horizontal polarization can be found in [1]. Due to the small storage capacity of the Elliott 503 computer, it was necessary to simplify solution to a great extent. The same solution has been derived from more general assumptions in [2] and therefore it offers the other possibilities (it has been shown that both horizontal and vertical polarization can be computed). Two different programs are described in [3]. The first program is intended for radar coverage pattern calculations, when the observation point  $P$  in the infinite distance is considered. The second program calculates a propagation factor over the irregular terrain for the finite distance between the antenna and the observation point  $P$ . These programs differ from [1] because they allow to compute propagation over irregular terrain for both horizontal and vertical polarization considering the Fresnel reflection coefficient for terrain with random deviations and refraction (it is possible to enter the effective earth radius). To compute reflections, the contributions from the irregular terrain are integrated. That cannot be used, if the difference between the incident and reflected rays is too small. For the difference less than one third of the wavelength, the electric field is computed using very simplified assumptions (see [3], Eq. (7)). The computer model and computation accuracy for propagation over irregular terrain has been presented [4], where the special attention is paid to computation for low altitude propagation and the finite distance between the antenna and the observation point (diffraction field zone). Comparing with [3] the more accurate solution is described for this case. Various cases of electromagnetic wave propagation over irregular terrain have been solved. The programs have been successfully used for analyses and selections of antenna far-field measurement ranges and radar sites. Computations, measurements and published solutions for individual special cases agree quite well (some comparisons are given in [1] to [4] and [9]). That demonstrates the usefulness of the described method.

It is said that the physical optic method, which is used in [1] to [4], is very time consuming. The crucial problem is the numerical integration method selection. Usually the sampling theorem is applied automatically and it is stated that it is necessary to use the half wavelength step size for numerical integration. In fact, the integration step selection is not a simple problem. Sometimes, the integration step should be chosen smaller (such as [5]). On the other hand, the half wavelength step is not usually necessary. That was shown in [1] using the generalized trapezoidal method [6]. Similarly, the effect of terrain reflection for vertical dipole considering the integral equation

and the simplification using more effective integration has been shown [7]. The simplified calculation of antenna electric field over the irregular terrain has been proposed [8], which uses the linear piecewise approximation of the terrain and the simple Fresnel integral approximation. That reduces the calculation amount substantially and enables both the analysis and synthesis of irregular terrain effects. The comparison of the methods [8] and [1] is given in [9].

The selection of integration step (subinterval) is rather complicated question. That is demonstrated using numerical simulations for various wavelengths for the generalized trapezoidal method [6].

## 2. Propagation over irregular terrain

Let us consider the antenna  $A$  over the earth surface as shown in Fig. 1. If the difference between the incident and reflected rays is greater than one third of the wavelength, the method described in [3] is used. The vector of electric field  $\mathbf{E}$  at the point  $P$  is given by

$$\mathbf{E}(P) = \mathbf{E}_i(P) + \mathbf{E}_s(P) \quad (1)$$

where:

- $\mathbf{E}(P)$  ..... resultant electric vector,
- $\mathbf{E}_i(P)$  ..... incident electric vector,
- $\mathbf{E}_s(P)$  ..... scattering electric vector.

According to [2], the following relationship can be derived

$$\frac{E_s(P)}{|E_0|} = \frac{R_0 e^{j\pi/4}}{\sqrt{\lambda}} \int_{-\infty}^{\infty} f(\theta_1) \left[ \frac{1-\tilde{A}}{2} \sin(\theta_1 - \alpha) + \frac{1+\tilde{A}}{2} \sin(\theta_2 - \alpha) \right] \frac{e^{-jk(R_1+R_2-R_0)}}{\sqrt{R_1 R_2 (R_1+R_2)}} dx \quad (2)$$

where:

- $R_0, R_1, R_2, \theta_1, \theta_2, \alpha$  ..... are shown in Fig. 1,
- $f(\theta_1)$  ..... normalized antenna radiation pattern,
- $A$  ..... phase center of antenna in the point,
- $h_A$  ..... height over earth terrain,
- $\Gamma$  ..... reflection coefficient,
- $k = 2\pi/\lambda$ ,
- $\lambda$  ..... wavelength.

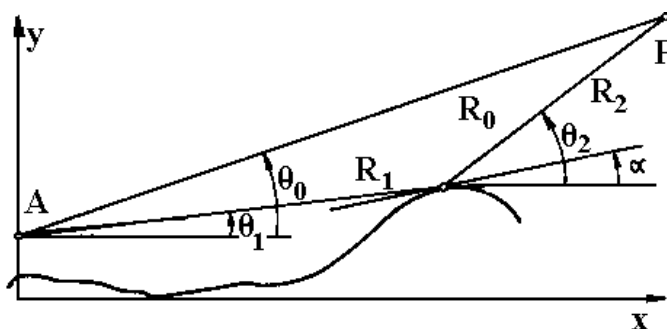


Fig. 1 Propagation over terrain geometry

The reflection coefficient for surface with the random deviations is given by

$$\Gamma = \Gamma_0 \exp [-2(2\pi\sigma \sin \gamma_0/\lambda)^2] \quad (3)$$

where:

- $\sigma$  ..... surface standard deviation,
- $\Gamma_0$  ..... Fresnel reflection coefficient of smooth surface,
- $\gamma_0$  ..... reflection angle.

The reflection angle is the angle between the tangent and the incident (reflected) ray. For calculation, the surface points are read - the length of arc  $r_B$  and height  $h_B$  according to Fig. 2.

The coordinates  $(x_B, y_B)$  are given by the following expressions

$$\begin{aligned} x_B &= (R_e + h_B) \sin \alpha_z \\ y_B &= (R_e + h_B) \cos \alpha_z - R_e \\ \alpha_z &= x_B / R_e \end{aligned} \quad (4)$$

where:

$R_e$  ..... effective earth radius.

The effective earth radius is usually chosen  $R_e = 8500$  km. The shadow (non-illuminated earth) is considered according to Fig. 3

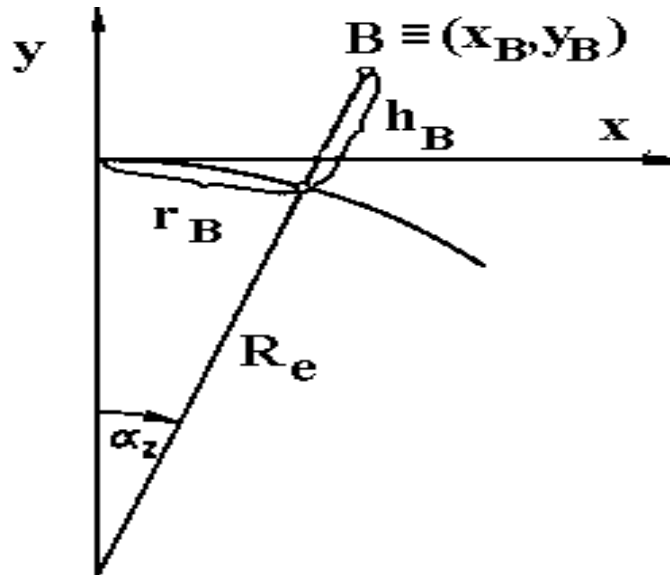


Fig. 2 Curvature correction

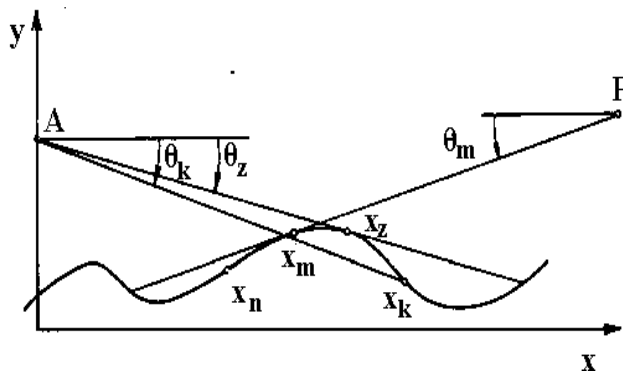


Fig. 3 Shadow areas

For the first type of shadow (point  $x_k$ ), the following expression is obviously valid

$$\begin{aligned} \theta_k &< \theta_z \\ \text{for } x_k &> x_z \end{aligned} \quad (5)$$

For the second type of shadow (point  $x_k$ ), the following expression is held

$$y_m > y_n + (x_m - x_n) \tan \theta_m \quad (6)$$

### 3. Computation

The calculation of (2) is rather difficult problem. Firstly, the terrain profile should be approximated using the terrain digital model. Then the coordinates  $(x_B, y_B)$  are evaluated using (4). The reflection coefficient can be calculated using the Fresnel reflection coefficient and (3). The zero shadow area amplitude can be considered (that is strictly valid for infinity obstacle radius). It has been shown [3] that is the acceptable assumption even for the two knife-edge obstacles.

Then it is necessary to select the suitable numerical integration method, integration interval and step for numerical integration. The  $(x_A, x_B)$  integration interval can be chosen, where  $x_A$  is antenna coordinate and  $x_B$  is maximum illuminated distance.

The crucial problem is the numerical integration method selection. Any integration method is limited. Due to finite number of integration points (sampling), the aliasing is created for Fourier transform, when any frequency component outside of the frequency range is aliased into that range. Generally, their effect will be diminished using smaller integration steps. It has been proved that the generalized trapezoidal method [6] can be successfully used. The analysis of integration steps for the used method has been performed and some examples such as cosine antenna illumination with quadratic phase error have been given [6]. This analysis cannot be used for the real terrain because of the complexity of the problem. It seems that the only solution is to consider various typical cases. Several cases of terrain have been considered for numerical studies.

Numerical simulations have been performed for various profiles and wavelengths. Both plane and irregular terrain ground profiles have been observed. The normalized electric field  $|E/E_0|_N$  has been computed, where  $E$  is given by (1),  $E_0$  is the maximum value of  $E_r$  at distance  $R_0$  (for the maximum value of the radiation antenna pattern),  $|E/E_0|_N$  are values calculated using integration steps of  $N$  meters. Let us consider that the ground surface is formed by horizontal plane except the part shown by Fig. 4. The A profile is the plane ground surface, the depressions form the profiles B and C and the hill creates the D profile.

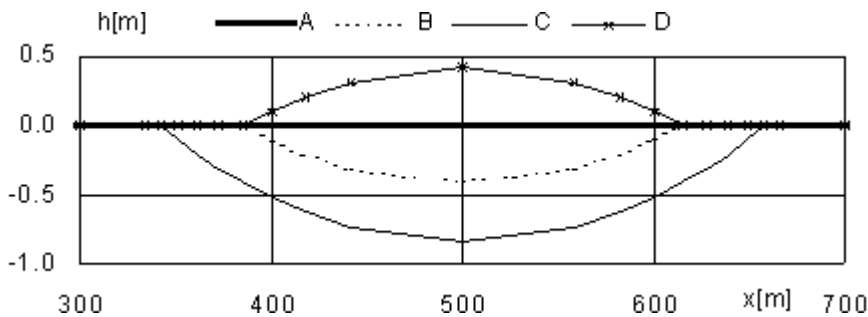


Fig. 4 Differences  $h[m]$  between the plane and profiles A, B, C and D

The values  $|E/E_0|_N$  for  $N$  equals 1, 10 and 20 m, the plane ground surface (A profile), antenna height  $h_1 = 10$  m, the wavelength  $\lambda = 0.1$  m and  $R_0 = 1$  km (the distance between antenna and point  $P$ ) are shown in Fig. 5. It can be seen that the values  $|E/E_0|_N$  are slightly different for various integration steps  $N$ . It is clear that these results can be practically used regardless of integration step (subinterval size 1 to 20 m). That means that integration step size can be 10 to 200 times greater than wavelength.

Naturally, the Fig. 5 and various numerical simulations cannot be considered as a verification of some general rule. The values  $|E/E_0|_N$  have been computed for heights  $h_1$  equal 10 and 15 m, the A, B, C and D profiles, wavelengths equal 0.1, 0.03 and 0.01 m, values  $N$  are equal to 1, 2, 5, 10 and 20 m and  $R_0 = 1$  km. Therefore, the following examples can be only considered as a demonstration of some general conclusions. The differences  $\Delta_N = |E/E_0|_1 - |E/E_0|_N$  are shown in Fig. 6 to 8 for various  $N$ , profiles and wavelengths.

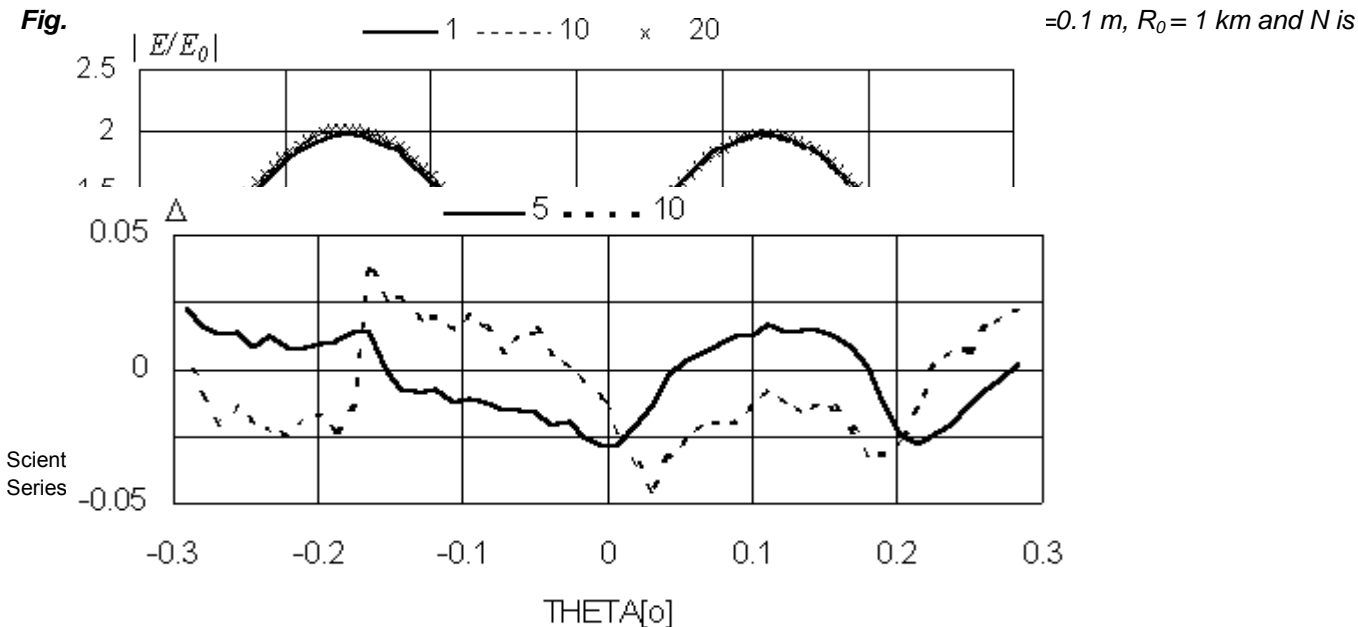
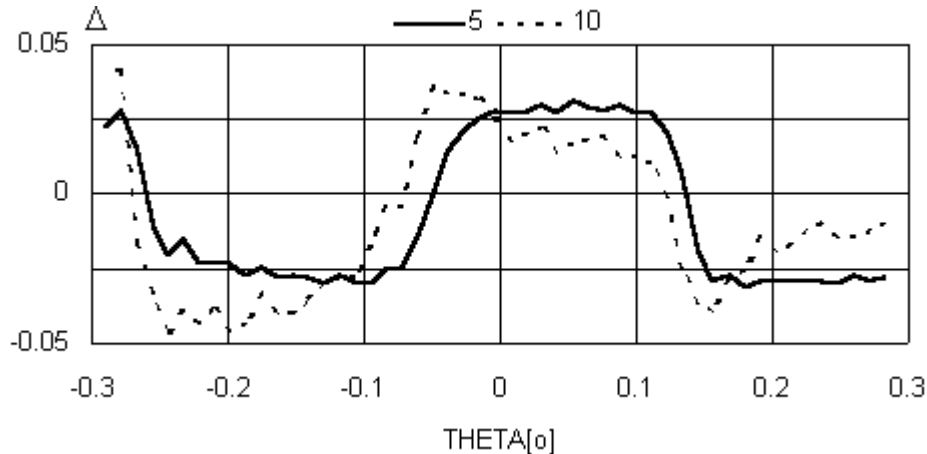


Fig.  $|E/E_0|$  — 1 — 10 — x — 20  $\Delta_N = |E/E_0|_1 - |E/E_0|_N$  — 5 — 10  $\lambda = 0.1$  m,  $R_0 = 1$  km and  $N$  is

**Fig. 6** Differences  $\Delta_N = |E/E_0|_1 - |E/E_0|_N$  for  $N=5$  and  $10$  m, C profile,  $h_1=15$  m,  $\lambda=0.1$  m and  $R_0=1$  km

The terrain effect (C profile depression and D profile hill) is demonstrated in Fig. 6 and 7 for wavelength  $\lambda=0.1$  m,  $h_1=15$  m and  $R_0=1$  km. Due to fact that the character of resultant electric fields is quite different for the C and D profiles (the maximums and minimums of electric field for C profile are more express than for D profile and their positions are different), the differences  $\Delta_N$  are not similar. However, their significance is comparable. The wavelength effect (wavelengths 0.1 and 0.03 m) is demonstrated in Fig. 6 and 8 for C profile,  $h_1=15$  m and  $R_0=1$  km.



**Fig. 7** Differences  $\Delta_N = |E/E_0|_1 - |E/E_0|_N$  for  $N=5$  and  $10$  m, D profile,  $h_1=15$  m,  $\lambda=0.1$  m and  $R_0=1$  km

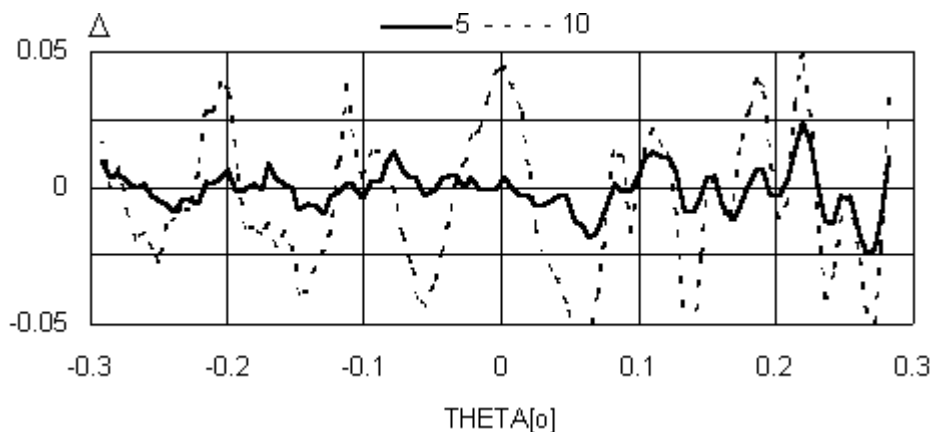


**Fig. 8** Differences  $\Delta_N = |E/E_0|_1 - |E/E_0|_N$  for  $N=5$  and  $10$  m, C profile,  $h_1=15$  m,  $\lambda=0.03$  m and  $R_0=1$  km

The computed cases have demonstrated that the simple general rules cannot be stated. The effects of integration method and another effects (such as terrain shape) are presented. Even the effect of used wavelength is not unambiguous. It is clear that the character of error behavior depends on the wavelength. If the wavelength is greater, the integration steps can be greater considering the quadratic phase errors. On the other hand, if the wavelength is greater, the Fresnel zone dimensions increase and therefore the phase for majority of surface is constant. The phase is changed very quickly near by the boundaries of integration interval and the greater steps cause the error [1]. That is very pronounced for plane segments (especially for reflection near by edges, i.e. for very low or very high angles  $\theta_0$ ). Therefore, it is not possible to increase the integration steps according to the wavelengths linearly because of the described phenomena and the reasonable compromise between the accuracy and the number of integration points (time of computation) should be chosen. This compromise cannot be taken as the fixed general rule.

According to the numerical simulations for various wavelengths and terrain profiles, the integration step of 5 or possibly 10 m for the wavelength of  $\lambda=0.1$  m can be recommended. The integration step of 10 m is not suitable for shorter wavelengths. The suitable integration step for the wavelength of  $\lambda=0.03$  m is 5 m and for the wavelength

of  $\lambda=0.01$  m is 2 m. It is clear that the sampling theorem cannot be applied automatically because these steps are substantially greater than  $\lambda/2$ . Except the wavelength, the digital terrain model should be considered because the integration step should be smaller than the smallest horizontal segment. If the terrain profile is very complicated, it may be useful to halve the integration steps and compare the obtained results. In case that the results are substantially different, the new integration step should be chosen.

#### 4. Conclusions

The computer model and computation accuracy for propagation over irregular terrain are presented. The model differs from [1] because it allows to compute propagation over irregular terrain for both horizontal and vertical polarization considering the Fresnel reflection coefficient for terrain with random deviations and refraction (it is possible to enter the effective earth radius). To compute reflections, the contributions from the irregular terrain are integrated. That cannot be used, if the difference between the incident and reflected rays is too small. Computation results obtained by described method agree quite well with the calculations of special cases and measurements.

The paper describes the effect of integration step selection for various wavelengths and profiles. According to the numerical simulations for various wavelengths and terrain profiles, the recommendations for integration step selection are given. It can be concluded that the sampling theorem cannot be applied automatically because these steps are substantially greater than  $\lambda/2$ .

*Lektoroval: Prof. Ing. Miloš Mazánek, CSc.*

Předloženo v únoru 2001.

## References

- [1] Schejbal, V.: Computing the electric field strength of an antenna above an irregular earth (in Czech). Slaboproudý obzor, Vol. **34**, 1973, no. 12, pp. 541 - 547.
- [2] Kupčák, D.: ATC radar antennas. Environment influence on ATC radar operation (in Czech). Praha MNO, 1986, Vol. III, Chap. 16 - 18.
- [3] Schejbal, V.: The earth influence on the electric field of antenna (in Czech). Slaboproudý obzor, Vol. **52**, 1991, no. 9 - 10, pp. 218 - 224.
- [4] Schejbal, V.: Propagation over irregular terrain. Radioengineering, Vol. **6**, 1997, no. 1, pp. 19 - 22.
- [5] Schejbal, V. - Hönl, J.: Holographic method of near-field antenna measurements. 10th European Microwave Conference, Warszawa, 1980, pp. 167 - 171.
- [6] Kupčák, D.: Evaluation of antenna radiation patterns by the generalized trapezoidal method. Tesla Electronics, **7**, 1974, no. 2, pp. 43 - 50.
- [7] Akorli, F. - Costa, E.: An efficient solution of an integral equation applicable to simulation of propagation along irregular terrain. Millenium Conference on Antennas and Propagation. Davos, April 9 - 14, 2000. Abstracts Volume II, pp. 44, CD ROM (full paper).
- [8] Schejbal, V.: Simplified calculation of antenna electrical field over irregular terrain (in Czech). Slaboproudý obzor, Vol. **41**, 1980, no. 11, pp. 545 - 547.
- [9] Schejbal, V.: Some remarks on the propagation of electromagnetic waves in the range of 1 to 20 GHz (in Czech). Slaboproudý obzor, Vol. **44**, 1983, no. 7, pp. 328 - 333.

## Resumé

### PŘESNOST VÝPOČTŮ ŠÍŘENÍ ELEKTROMAGNETICKÉ VLNY NAD NEROVNÝM TERÉNEM

Vladimír SCHEJBAL

Příspěvek uvádí počítačový model a přesnost výpočtů šíření vln nad nerovným terénem. Stručně je popsána metoda výpočtu pomocí fyzikální optiky, která umožňuje uvažovat jak vertikální, tak i horizontální polarizaci, vlastnosti reálného terénu (komplexní permitivitu, permeabilitu a drsnost povrchu), zastínění povrchu, index lomu atmosféry a charakteristiky vysílací antény. Zvláštní pozornost se věnuje přesnosti s uvážením numerické integrace a velikosti kroku. Vliv volby integračního kroku pro různé vlnové délky a terénní profily se demonstruje pomocí numerické simulace pro různé frekvence a nerovné terény. Je ukázáno, že není nutné používat vzorkování podle vzorkovacího teorému, ale postačí podstatně méně vzorků. Přitom velikost vzorkování není úměrná pouze použité délce vlny, ale je ovlivněná i tvarem terénu.

## Summary

### COMPUTATION ACCURACY OF ELECTROMAGNETIC WAVE PROPAGATION OVER IRREGULAR TERRAIN

Vladimír SCHEJBAL

The computer model and computation accuracy for propagation over irregular terrain are presented. Special attention is paid to computation accuracy considering numerical integration and step size. The effect of integration step selection for various wavelengths and terrain profiles is demonstrated using numerical simulations.

## Zusammenfassung

### BERECHNUNGSGENAUIGKEIT DER AUSBREITUNG DER ELEKTROMAGNETISCHEN WELLE OBERHALB EINES UNEBENEN TERRAINS

Vladimír SCHEJBAL

Der Beitrag beschreibt den Rechenmodel und die Berechnungsgenauigkeit der Ausbreitung der elektromagnetischen Wellen oberhalb eines unebenen Terrains. Besondere Aufmerksamkeit wird der Genauigkeit rücksichtlich der numerischen Integration und der Schrittengröße gewidmet. Der Einfluß der Integrationsschrittwahl für verschiedene Wellenlänge und Terrainprofile wird mittels numerischen Simulation demonstriert.